

# Microstructure evolution upon annealing of accumulative roll bonding (ARB) 1100 Al sheet materials: evolution of interface microstructures

Charles Kwan · Zhirui Wang

Received: 26 October 2007 / Accepted: 25 March 2008 / Published online: 9 April 2008  
© Springer Science+Business Media, LLC 2008

**Abstract** The microstructure evolution upon annealing of 1100 aluminum samples that were accumulative roll bonding (ARB) processed were studied with the use of transmission electron microscopy. It was found that the ultra-fine microstructure resulted from the ARB process was not stable. Specifically, a two-stage grain growth behavior was observed, in which a relatively slower rate of grain growth was followed by a more rapid grain growth rate at higher annealing temperature. The bonding interfaces that were unique to the roll bonding process were found to have a significant influence on the grain growth behavior when the grain size of the material was of similar dimension as the bonding interface separation. Discontinuous pockets consisting of smaller grains were found to have formed upon annealing. These pockets represented the remnants of the heavily deformed layer from wire brushing.

## Introduction

The desire to obtain ultra fine (UF) grained materials, i.e. materials with grain size in the submicron range, for improvement of material strength has long been the driving force for the development of procedure(s) to produce UF grained material in bulk quantities. In recent years, Saito et al. [1, 2] successfully applied a procedure named accumulative roll-bonding (ARB) to produce UF-grained

materials. The procedure involved the passing of two sheets, one sheet stacked securely on top of the other, through a set of rollers to achieve a 50% reduction in the sheet thickness. With the proper surface treatments, such as degreasing and surface contaminates removal with the use of a steel wire brush prior to the stacking of the two sheets, a sound bond can be formed between the two sheets after the rolling pass [3, 4]. The product after the rolling pass were cut into halves and subjected to the same rolling process once again. This procedure can be done repeatedly as desired. The reduction ratio of each pass does not need to be set at 50%, although a certain threshold reduction ratio must be surpassed to assure a sound bond [5]. However, 50% would results in a constant thickness after any given number of passes. The ARB process has been demonstrated to be able to produce UF grained sheets of various aluminum alloys [6–16], copper and copper alloys [17–19], and even interstitial free steels [20].

One of the concerns with adapting UF grained material for practical uses is the lack of ductility that the product exhibits. The logical solution to this dilemma is the use of proper postprocess treatment such as annealing. Obviously, the knowledge of microstructure evolution upon annealing of ARBed materials is a critical part of our understanding of microstructure–property relationship of this type of materials for their practical applications. The focus of the present study was therefore set to evaluate systematically such microstructure evolution upon annealing of ARBed 1100 series commercial-purity aluminum materials after different number of ARB cycles by using transmission electron microscopy (TEM). Effort has also been placed in the observation of microstructure evolution of the layer interfaces embedded within ARB material. The layer interfaces contain oxide particles that had originated from the oxide film formed on the faying surface, which can be

---

C. Kwan · Z. Wang (✉)  
Department of Materials Science and Engineering, University  
of Toronto, Toronto, ON, Canada  
e-mail: zhirui.wang@utoronto.ca

detrimental to mechanical properties. The number of interfaces increases exponentially with the number of passes performed in the ARB process, and hence the number of interfaces is quite large in ARB materials. It is, therefore, important to point out that any detrimental effect arriving from each individual interface will magnify significantly with the increase in the number of interfaces. The present investigation also attempted to explore the effect of such interfaces on microstructure evolution.

### Experimental procedure

Sheets of 1100 commercial-purity aluminum with a thickness of 1 mm were used as the base material for this study. The aluminum sheets were first heat treated to a fully annealed condition by annealing at 400 °C for 1 h. The intended bonding surfaces on each sheet were degreased with acetone and wire brushed with a steel wire brush. The two sheets were then stacked one on top of the other and secured tightly together by steel wires at the corners of the assembled sheets. The assemblage was then cold rolled to a 50% reduction. This procedure was then repeated up to eight times. Samples investigated in this study were obtained after four cycles, six cycles, and eight cycles of the ARB process. Post-ARB annealing was done in an air furnace with annealing temperature ranging from 100 to 600 °C for 1.8 ks.

Microstructure analyses were carried out using a Hitachi H-800 Transmission Electron Microscope (TEM) with an accelerating voltage of 200 kV. TEM thin foil samples were prepared using twin-jet electro-polishing with an electrolyte consisting of a ratio of 1:2 nitric acid to methanol. Grain size measurements were carried out by measuring at least 200 grains from three distinctive micrographs for each set of samples. Optical microscopy (OM) was also performed on selected samples where TEM analysis was deemed unsuitable. OM samples were electrolytically etched with an electrolyte consisting of 4%  $\text{HBF}_4$  at 30 V.

### Results and discussion

#### Microstructure evolution upon annealing

The micrographs of the eight cycles samples after annealing at different temperatures are shown in Fig. 1. The micrographs of the six cycles and four cycles samples upon annealing are presented in Figs. 2 and 3, respectively. A summary of the mean grain size of four cycles, six cycles, and eight cycles sample upon annealing at different temperature is presented in Fig. 4.

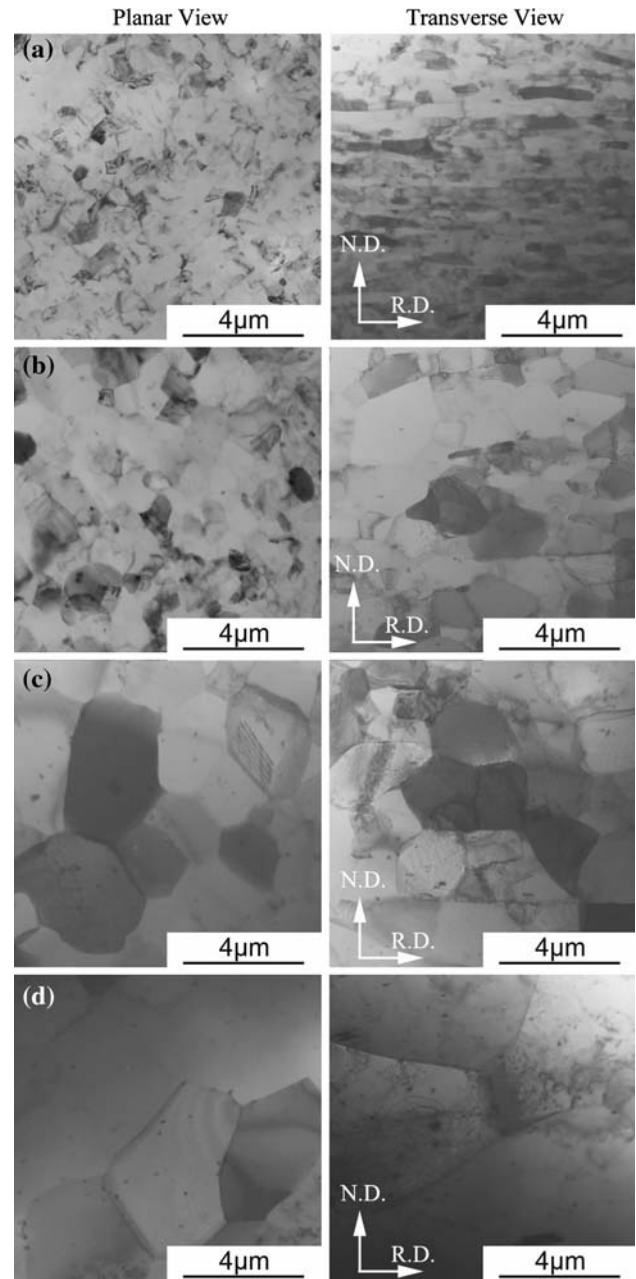


**Fig. 1** Bright field TEM micrographs of eight cycles samples (a) in the as rolled condition, and annealed at (b) 200 °C, (c) 250 °C, and (d) 400 °C for 30 min

The microstructure of all of the samples of the as-rolled condition observed in the current study consisted of pancake-shaped UF grains surrounded mostly by high-angle boundaries, as shown in Figs. 1a, 2a, and 3a. Such observations of grains surrounded by high-angle boundaries as well as the low-dislocation density within the grains for such a severely plastic deformed material was consistent with that of a dynamically recovered structure. Similar observations of a dynamically recovered structure were also reported in previous studies on ARB materials,

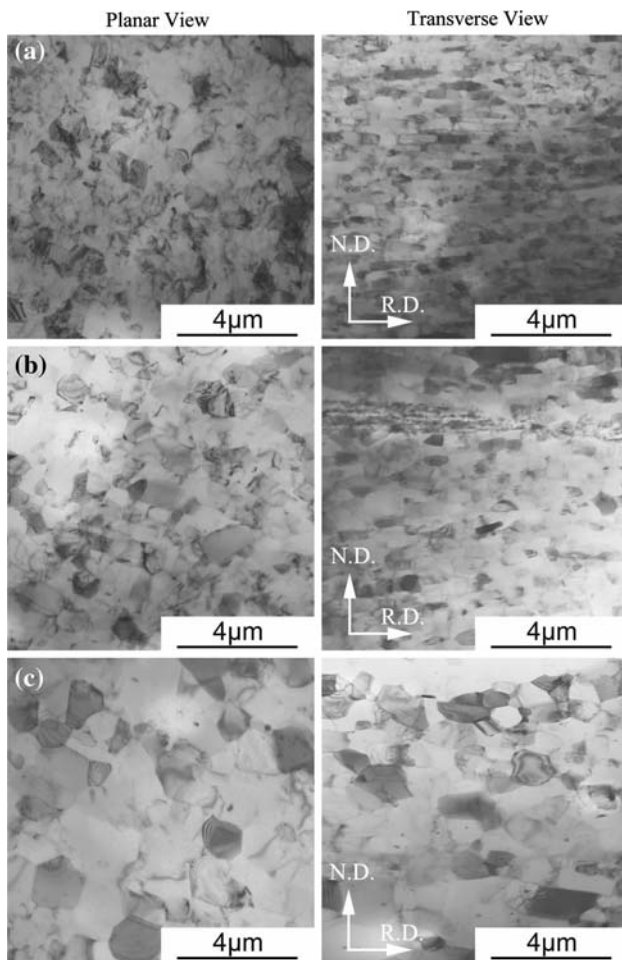


**Fig. 2** Bright field TEM micrographs six cycles samples (a) in the as-rolled condition, and upon annealing at (b) 150 °C, and (c) 200 °C

specifically in [10–16] for 1100 series aluminum. There were no noticeable changes in the mean grain size of the as-rolled samples after the various numbers of cycles of ARB tested in this study.

Recovery and grain growth occurred upon annealing of the as-ARB materials. However, it should be noted that from both qualitative study of the micrographs by comparing Figs. 1–3, and quantitative analysis through grain size measurements by comparing the results in Fig. 4, one could not detect any apparent stage of recrystallization. Note that the lack of recrystallization stage for ARB 1100 aluminum was also reported in [13]. However, Kamikawa et al. have reported recrystallization in their ARBed 4 N pure aluminum [14]. In the present investigation, instead, what was found is the continuous growth of the grains even at very low annealing temperature, suggesting that the microstructure was not stable. Upon temperature increase up to the annealing temperature of 200 °C, the grain growth rate was comparatively slow. It should also be noted that, at annealing temperatures below 200 °C, grain boundary migration rate,

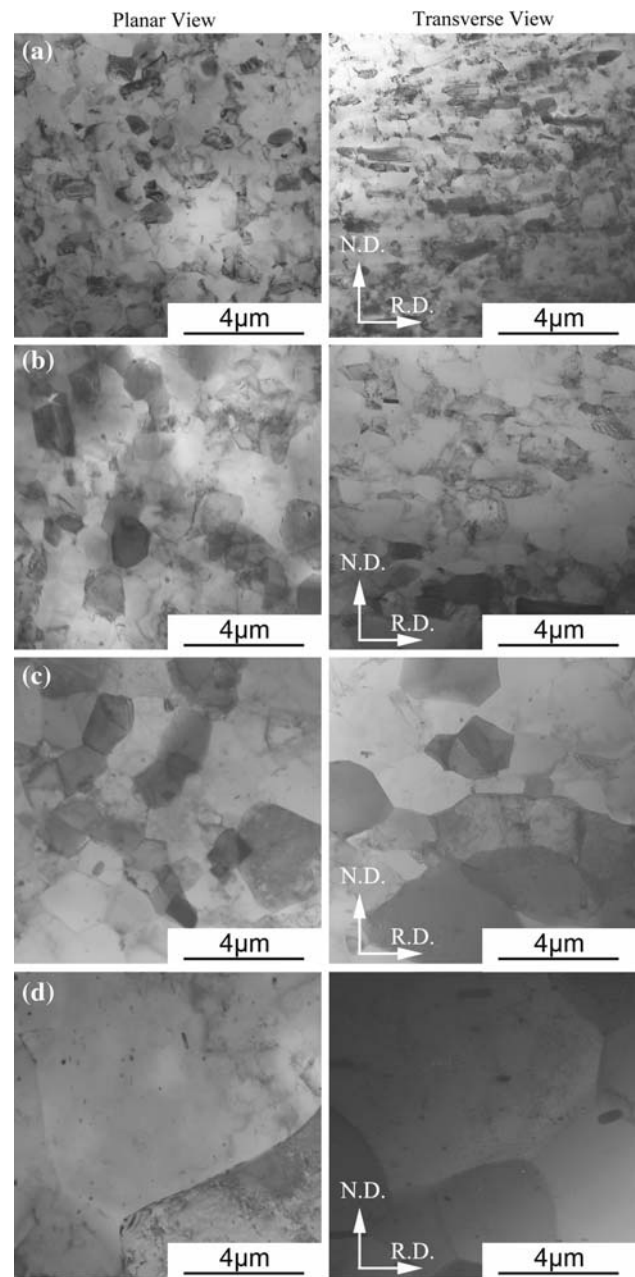


**Fig. 3** Bright field TEM micrographs four cycles samples (a) in the as-rolled condition, and upon annealing at (b) 200 °C, (c) 250 °C, and (d) 300 °C

as estimated from the slope of the grain size versus annealing temperature curves in Fig. 4, in both the direction parallel to the rolling direction and the direction perpendicular to the rolling direction were found to have a similar rate until the grains had reached an equiaxed geometry at an annealing temperature of 250 °C. Coincidentally, at annealing temperatures slightly below 250 °C, rapid grain growth was indeed observed to have begun.

In the present work, it was also noticed that the grain growth behavior upon annealing was influenced by the



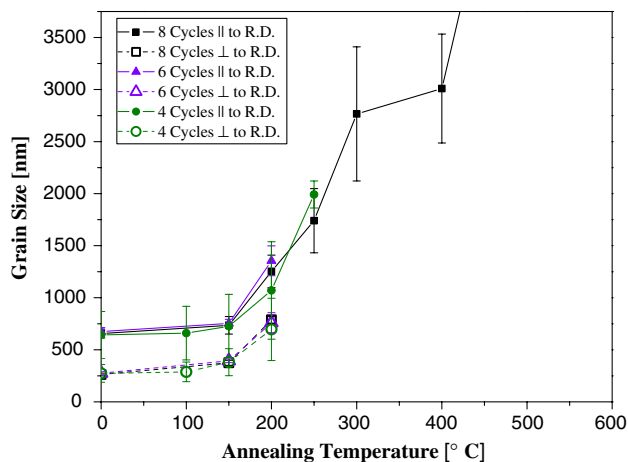


**Fig. 4** Comparison of grain sizes of four, six, and eight cycles samples upon annealing at different temperature for 30 min

bonding interfaces introduced in the rolling process. Such an effect was most prominently shown in the grain growth progress and grain size development of the eight cycles samples when annealed at 300 and 400 °C. As can be seen in Fig. 4, under such annealing conditions, the grains of the eight cycles samples have been flattened to a value of approximately 3  $\mu\text{m}$  and these grains eventually grew steeply to a conventional grain size that was similar to the base material when the samples were annealed at 600 °C. This phenomenon was clearly demonstrated when optical micrographs of the transverse view of eight cycles samples annealed at 400 and 600 °C were compared, as shown in Fig. 5. It was interesting that some intact bonding interfaces can still be observed even after annealing the samples at 400 °C, as shown (*arrowed*) in Fig. 5d. The afore-described microstructures, specifically the fact that there was a lack of significant grain growth between 300 and 400 °C, represent a relatively stable microstructure status. It was apparent that grain boundary migration had been retarded by the existence of the bonding interfaces. Cao et al. has also observed this phenomenon and have suggested that the rolled-in oxide have caused Zener drag hence hindered the grain boundary migration across the bonding interface [9]. Upon annealing at higher temperature, the driving force for grain boundary migration has seemingly surpassed that of the Zener drag, hence leading to further growth. This further growth has led to some of the layer interfaces to be engulfed by the grain growth process and such an engulfing effect cannot be detected easily in most TEM samples. However, through a large amount of TEM investigation, it has been indeed observed in one of the TEM samples for the eight cycles 400 °C annealed material, as shown in Fig. 5d (*dashed arrows*). In Fig. 5d, the distance between the dashed arrows and the solid arrows at the lower right corner is about 4  $\mu\text{m}$ , a value almost equal to the theoretical interface separation

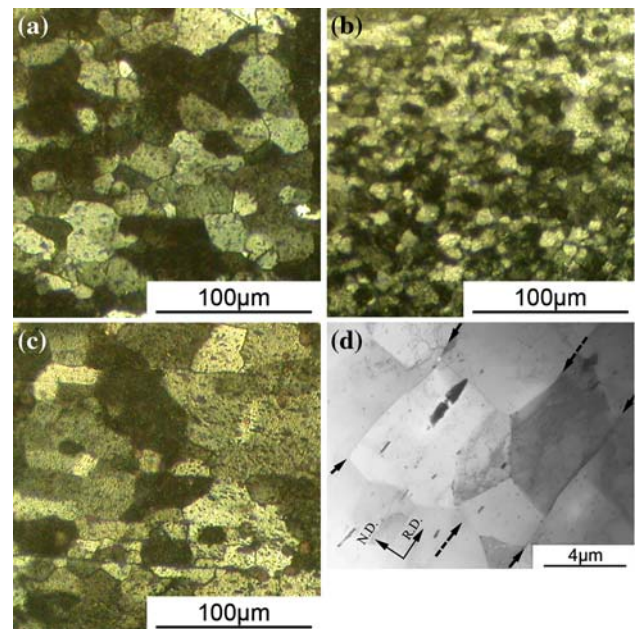


**Fig. 5** Optical micrographs of (a) base 1100 Al sample, eight cycles sample upon annealing at (b) 400 °C, (c) 600 °C, and (d) TEM micrograph of eight cycles samples upon annealing at 400 °C showing the restriction of grain growth by the still intact bonding interfaces (*arrowed*) as well as an interface that has been engulfed by grain growth (*dashed arrows*)

distance. Although the dashed arrows in Fig. 5d do not indicate a clear interface, the existence of the interface is evidenced by the faint line from the grain beneath the TEM foil surface indicated by the dashed arrows. The retardation of grain growth due to Zener drag was expected to be present for all of the samples regardless of the number of cycles of ARB it had gone through. However, since the bonding interface separation for the other samples were relatively large compared to the grain size it would have reached upon annealing at 300 and 400 °C, such an effect was not noticeable in the grain size data.

**Microstructure evolution upon annealing of the immediate surrounding to the bonding interfaces**

The surrounding of the bonding interfaces are expected to show specific features in its microstructure due to: (1) the microstructure created due to the bonding mechanism—a severe plastic deformation process, and (2) the intermixed oxide layer and dispersoids that were formed before roll-bonding.

It was interesting that the bonding interface appears similar in most as-rolled samples and it was mostly in the form of a single long straight grain boundary. Such a long boundary borders all the grains on the two sides of the interface, as arrowed in the TEM micrograph in Fig. 6a. However at some interfaces, pockets of heavily strained

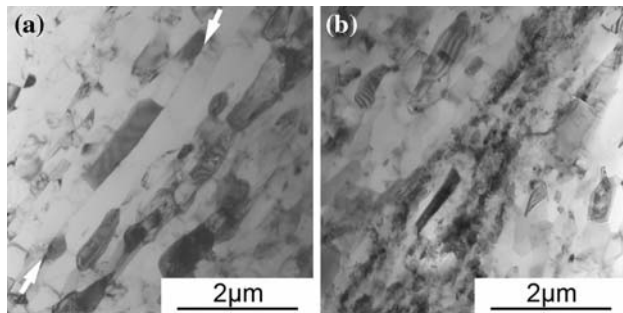


**Fig. 6** Bright field TEM micrographs of an eight cycles as-rolled sample showing the morphology of a bonding interface under the TEM

material, consisting of heavily worked structure, have also been observed. Similar observation was reported by Tsuji in [21] as well. It should be noted that both form of layer interfaces shown in Fig. 6a and b existed in all ARB samples observed. These pockets appeared discontinuously along the bonding interfaces and the size and location of these pockets seem to be random. The heavily deformed material was thought to be under strong residual stresses and it has nanocrystalline grains, which are believed to have gone through a dynamic recovery process during ARB. Upon further annealing, on the other hand, the heavily strained material, which was not dynamically recovered, was observed to have now been through such a process in a massive way and have become crystalline. These microstructures are seen to have further grown during annealing. A typical example for this anomaly in the interface microstructure and its evolution upon thermal treatment is shown in Fig. 7 for a four cycles sample. It is interesting to point out that, qualitatively, the frequency of these pockets seems to be lower in the as-rolled materials compared to the annealed samples. This would suggest that some of these pockets may have been so small that it would not be noticeable in the as-rolled materials. However upon annealing, these pockets of heavily deformed region seem to increase in size.

The existence of these discontinuous regions of heavily deformed material along the bonding interfaces, a precursor to the pockets of fine elongated grains upon annealing, was due to the bonding mechanism of roll bonding process. Such anomalies were also reported by Vaidyanath et al. [22] on their traditional roll bonding experiments. Vaidyanath et al. argued that these regions were remnant of the heavily worked structure introduced to the faying surface during the wire-brushing stage [22]. They had also suggested that the discontinuity of these regions arised from the breaking up of the brittle surface layer on the faying surface, consisting of the heavily deformed layer and possibly an oxide layer, which was essential for bonding to occur [22]. This idea was later confirmed and shown by Bay [23]. The brittle surface layer was to be

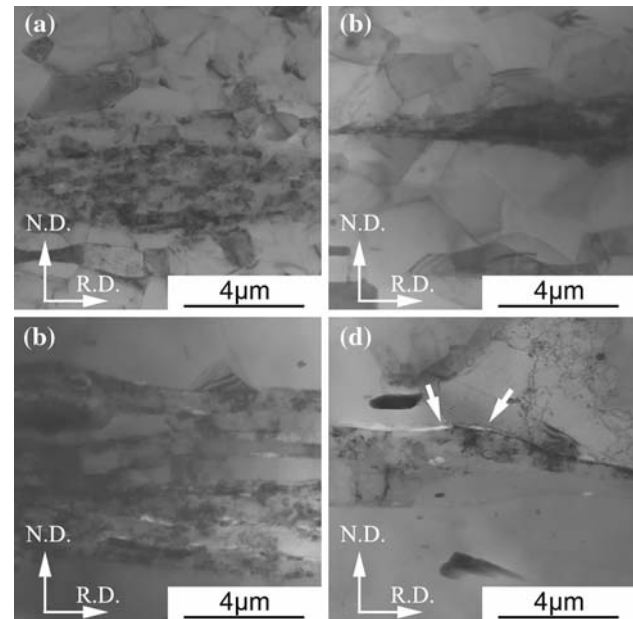


**Fig. 7** TEM bright field micrographs showing pockets of small grains located at the bonding interfaces in four cycles sample upon annealing at (a) 150 °C, (b) 200 °C, (c) 250 °C, and (d) 300 °C. Agglomerated second phase (most likely oxides) at the interface between the pockets and the matrix is arrowed

broken up upon surface expansion during roll bonding hence exposing the, protected, fresh metal underneath [23]. The exposed virgin metal, which was considered to be clean, was then extruded along and into the channel created by the broken up brittle surface layer and therefore made contact with the exposed virgin metal on the other faying surface. The contact of fresh clean metal on both side then formed the bond between the sheets [23]. As can be seen, it was due to the nature of the bonding mechanism that promoted the formation of discontinuous pockets of heavily deformed regions at the bonding interfaces.

On the other hand, contradictory to the results of Vaidyanath et al. [22], these regions of heavily deformed microstructure were seen less frequently in the as-rolled samples in the present study. This was possibly due to the cold rolling temperature used in the ARB process to subdue any possibility of grain growth. At the same time, the multiple times that the workpiece have passed through the rollers to high reduction might also have an influence on the phenomenon. As the number of cycles of ARB increases, the thickness of the heavily deformed layer would be comparable with the separation distance of adjacent bonding interfaces, and (aside from the small amount near the bonding interfaces) would most likely have dynamically recovered with the rest of the structure to form the UF grained structure and becomes part of the bulk. Consequently, the appearance of the regions of smaller grains was subdued in the as-rolled condition. On

the other hand, as the oxide portion of the brittle layer on the faying surfaces was significantly thinner than the heavily deformed layer, its detection was much more difficult. Oxide particles were also assumed to have broken up and possibly dispersed during the wire-brushing stage.

Upon annealing of the ARB samples, the heavily deformed pockets were recovered into the regions of small grains seen in Fig. 7. Polygonization could also have been an alternative mechanism, as sometimes the elongation geometry of the rolled structure was found to still remain even after the matrix of the material have reached an equiaxed state, such as in the case of 250 °C annealed four and eight cycles samples, compare Figs. 7c and 3c. On the contrary, the geometry might have been maintained as a result of Zener drag of the oxide dispersoids that have arrived during the wire-brushing stage. More interestingly, the relative grain growth rate of the smaller grains in the pockets with respect to the matrix grains were similar between 200 and 250 °C, i.e. the mean grain size in the pockets in both cases were approximately 11–12% of the grain size of the matrix. This has suggested that the grain growth rate of the matrix and the pockets were of similar rates albeit the obvious differences in the grain size between them. It should be noted that during the grain growth process there was a lack of grain boundary migration activity between the pockets of small grains and the matrix, i.e. grain boundary migration from within the pockets of small grains toward the matrix or vice versa. This phenomenon was evidenced when comparing the microstructure of the matrix and the pockets of small grains as annealing temperature increased, as shown in Fig. 7. It was interesting that when annealing at higher temperatures (300–400 °C in this case), these pockets found at the bonding interface were completely engulfed by a few number of grains, as shown in Fig. 7d. This behavior would suggest the existence of a retarding species that lied at the interface between the pocket of small grains and matrix, and the retarding species in this case was most likely oxide dispersoids as both Cao et al. and Vaidyanath et al. have suggested in [9] and [22], respectively. The existence of a retarding species near the bonding interface, especially within the interior of the pockets of small grains, was illustrated with the agglomerated second phase (presumably oxide particles) seen in higher temperature annealed samples, e.g. arrowed in Fig. 7d. Although the volume fraction of these pockets appears small, it had been speculated in a previous study that the appearance of such a stronger (due to grain size strengthening and possibly strengthening from oxide dispersoids) component lying near a presumably weaker bonding interface could be detrimental to mechanical properties, specifically ductility, of the material [24].

## Conclusions

Through the detail study of the microstructure evolution upon annealing of 1100 aluminum samples after different number of cycles of ARB, the following remarks can be concluded:

- (1) The UF microstructure developed through the ARB process was found to be unstable upon thermal treatment, during which, however, a clear two-stage grain growth behavior was observed. The first stage consists of a relatively low grain growth rate, in which the growth rates in both directions, parallel and perpendicular to the rolling direction, were found to be similar. The second stage consists of a more rapid grain growth toward conventional grain size. The transition between the first and second stage lies between 200 and 250 °C, coincidentally at which the grains became equiaxed. It should also be noted that there were no apparent recrystallization stage.
- (2) Restriction of grain growth by the existence of the bonding interfaces were observed in the eight cycles samples when the grain size have reached a dimension that were comparable to the bonding interface separation distance. The cause behind the restriction was possibly due to Zener drag of the grain boundaries from the “rolled-in” oxide dispersoids at the bonding interface.
- (3) Upon annealing of the samples, pockets consisting of much smaller grains were observed at the bonding interfaces. It is believed that these pockets, which arrived from recovery or possibly polygonization of the heavily deformed brittle layer, developed owing to the wire brushing for the processing. The discontinuity of the pockets was due to the nature of the bonding mechanism in roll-bonding. There was also a lack of grain migration activities across the interface between the pockets and the matrix. The reason was evidenced by the noticeable oxide agglomerates formed at higher annealing temperature suggested the existence of oxide at the interface between the pockets and the matrix.

**Acknowledgements** The authors would like to acknowledge Dr. Suk-Bong Kang of The Korean Institute of Material Sciences for providing the samples used in this study. This project is funded by Natural Science and Engineering Research Council of Canada (NSERC).

## References

1. Saito Y, Tsuji N, Utsunomiya H, Sakai T, Hong RG (1998) *Scr Mater* 39:1221. doi:10.1016/S1359-6462(98)00302-9
2. Saito Y, Utsunomiya H, Tsuji N, Sakai T (1999) *Acta Mater* 47:579. doi:10.1016/S1359-6454(98)00365-6

3. Vaidyanath LR, Milner DR (1960) *Brit Weld J* 7:1
4. Clemensen C, Juelstorp O, Bay N (1986) *Metal Constr* 18:625
5. Nicholas MG, Milner DR (1961) *Brit Weld J* 8:375
6. Xing ZP, Kang SB, Kim HW (2004) *J Mater Sci* 39:1259. doi:[10.1023/B:JMSSC.0000013884.69611.72](https://doi.org/10.1023/B:JMSSC.0000013884.69611.72)
7. Xing ZP, Kang SB, Kim HW (2002) *Metall Mater Trans A* 33:1521. doi:[10.1007/s11661-002-0074-9](https://doi.org/10.1007/s11661-002-0074-9)
8. Lee S-H, Lee CH, Lim CY (2004) *Mater Sci Forum* 449–452:161
9. Cao WQ, Liu Q, Godfrey A, Hansen N (2002) *Mater Sci Forum* 408–412:721
10. Huang X, Tsuji N, Hansen N, Minamino Y (2003) *Mater Sci Eng A* 340:265
11. Kim Y-S, Lee T-O, Shin DH (2004) *Mater Sci Forum* 449–452:625
12. Tsuji N, Ito Y, Saito Y, Minamino Y (2002) *Scr Mater* 47:893
13. Tsuji N, Ito Y, Nakshima H, Yoshida F, Minamino Y (2002) *Mater Sci Forum* 396–402:423
14. Kamikawa N, Tsuji N, Huang X, Hansen N (2006) *Acta Mater* 54:3055
15. Kim H-W, Kang S-K, Tsuji N, Minamino Y (2005) *Acta Mater* 53:1737
16. Kim H-W, Kang S-K, Tsuji N, Minamino Y (2006) *Mater Sci Forum* 512:85
17. Jang YH, Kim SS, Han SZ, Lim CY, Kim CJ, Goto M (2005) *J Mater Sci* 40:3527
18. Jang YH, Kim SS, Han SZ, Lim CY, Kim CJ, Goto M (2005) *Scr Mater* 52:21
19. Lee SH, Han SZ, Lim CY (2006) *Key Eng Mater* 317–318:239
20. Tsuji N, Okuno S, Matsuura T, Koizumi Y, Minamino Y (2003) *Mater Sci Forum* 426–432:2667
21. Tsuji N (2006) In: Altan BS (ed) *Severe plastic deformation*. Nova Science Publishers, pp 545–565
22. Vaidyanath LR, Nicholas MG, Milner DR (1959) *Brit Weld J* 6:13
23. Bay N (1986) *Metal Constr* 18:369
24. Kwan C, Wang Z, Kang S-B (2007) *Mater Sci Eng A* 480:148. doi:[10.1016/j.msea.2007.07.022C](https://doi.org/10.1016/j.msea.2007.07.022C)